Supplemental Information

Supplemental Figure 1. Growth and intake trajectories from 6 to 12 weeks of age. Body weight increased progressively over time, with a clear rise from 6 to 12 weeks. Weekly weight gain was most pronounced between 9 and 10 weeks and gradually plateaued thereafter. In parallel, daily food and water intake remained relatively stable across the observation period, indicating that the increase in body mass was not accompanied by major changes in consumption. Samples (heart, liver, kidney, blood, blood, urine, intestinal content, microbiome) were collected at 8, 10, and 12 weeks (red arrows). Data are shown as mean ± SEM for weight, and mean ± SD for weight increase. (created with BioRender.com)

Supplemental Figure 2. Organ-specific Gene Set Enrichment Analysis (GSEA) reveals distinct metabolic and functional transitions between 8 and 12 weeks. **(a)** Heart tissues exhibit up-regulation of pathways related to sarcoplasmic reticulum and calcium signaling, while oxidative phosphorylation and respiratory chain components are down-regulated, indicating a transition toward a maintenance-focused cardiac phenotype. **(b)** Kidney tissues display strong activation of immune-related pathways and antigen binding, suggesting progressive colonization by immune cell populations, alongside a down-regulation of Rac signaling-related pathways. **(C)** Liver tissues show a significant up-regulation of fatty acid metabolism and proteasome-related pathways, contrasted by a marked down-regulation of extracellular matrix organization and collagen-related structural components, reflecting the completion of hepatic structural maturation. Depicted is the negative log(10) of the adjusted p-value ($-\log_{10}$ adjust. p-value). (Red bars indicate up-regulated pathways; blue bars indicate down-regulated pathways; BP, Gene Ontology Biological Process; CC Gene Ontology Cellular Component; H, Hallmark; MF, Gene Ontology Molecular Function; R, Reactome).

Supplemental Figure 3. Heatmap visualization of differential gene expression in the heart, kidney, and liver during late adolescence. Comparison of gene expression enrichment profiles for respiratory chain/oxidative phosphorylation and fatty acid metabolism pathways. The heatmap illustrates organ-specific transcriptional adaptations. Notably, the heart displays down-regulation of oxidative phosphorylation components, while the kidney and liver show increased activity in fatty acid metabolic pathways. The heatmap depicts changes of differentially expressed genes identified by the GSEA terms GOCC_Respiratory Chain Comlex and KEGG_Oxidative Phoshorylation (Suppl. Table 1). Genes were aligned by hierachical clustering. Color scale represents normalized log FC2 values, with blue indicating low and red indicating high expression.

Supplemental Figure 4. Principal Component Analysis (PCA) of age-dependent metabolic shifts. (a) PCA of metabolomics data obtained from the intestine, plasma, and urine reveals distinct metabolic profiles, separating the time points 8, 10, and 12

weeks of age. The clear segregation of clusters in each matrix indicates systemic, age-dependent metabolic remodeling that occurs concurrently with the observed transcriptional changes during the transition to early adulthood. **(b)** Number of differentially regulated metabolites in intestine, plasma, and urine.

Supplemental Figure 5. Age-associated changes in short-chain fatty acids (SCFAs). Relative fold changes in cecal short-chain fatty acids (SCFA) levels determined by targeted analysis in 10- and 12-week-old mice in comparison to mice at 8 weeks of age are shown for 2-methylbutyric acid, isobutyric acid, isovaleric acid, hexanoic acid, propionic acid, valeric acid, acetic acid, and butyric acid. Bars indicate mean fold change. Asterisks denote statistically significant differences in comparison to levels at 8 weeks (adjusted p-value < 0.05). Overall, several SCFAs, including branched-chain fatty acids and classical fermentation products, were increased in older mice, consistent with age-dependent maturation of microbial metabolic activity.

Supplemental Figure 6. Hepatic ketogenesis. *Acsl1* (Acyl-CoA Synthetase Long-chain 1) activates long-chain fatty acids for both b-oxidation and lipid synthesis, increasing phospholipid, choline and sphingomyelin metabolites, while the Acyl-CoA thioesterases (*Acot2*, *Acot3*, *Acot8*) increase acylglycerols and lipid intermediates. Of note is the increased mitochondrial production of keton bodies (3-hydroxybutyroylglycine, 2S,3R-dihydroxybutyrate) and short- and medium chain fatty acids (butyrate/isobutyrate (4:0), 2-methylbutyrylcarnitine (C5), cis-4-decenoate (10:1n6)) liked linked to increased *Hmgc2* (3-Hydroxy-3-Methylglutaryl-CoA Synthase 2), *Hadha/Hadhnb* (Hydroxyacyl-CoA Dehydrogenase subunits), *Acadm* (acyl-CoA Dehydrogenase, medium chain). This is supported by peroxisomal breakdown of fatty acids, invovling *Ehhadh* (enoyl-CoA hydratase/3-hydroxyacyl-CoA dehydrogenase) and *Acaa1a/Acaa2* acitivty (acetyl-CoA acyltransferases).

Supplemental Figure 7. Temporal dynamics of microbial alpha diversity across intestinal niches. (a) Alpha diversity metrics, including observed richness, dominance, and Shannon diversity, were assessed in the small intestine, cecum, and feces of mice at 8, 10, and 12 weeks of age. Box plots depict the distribution of diversity indices at each timepoint. While the richness in the small intestine showed a progressive increase from 8 to 12 weeks, a downward trend was noted in the cecum. Richness in the feces increased from 8 to 10 week, followed by a slight decrease at 12 weeks. **(b)** Examples of bacterial changes in the small intestine and in the feces of mice between 8 and 12 weeks of age. Collectively, these observations illustrate the progressive changes in microbiome assembly as the mice mature.

Supplemental Figure 1

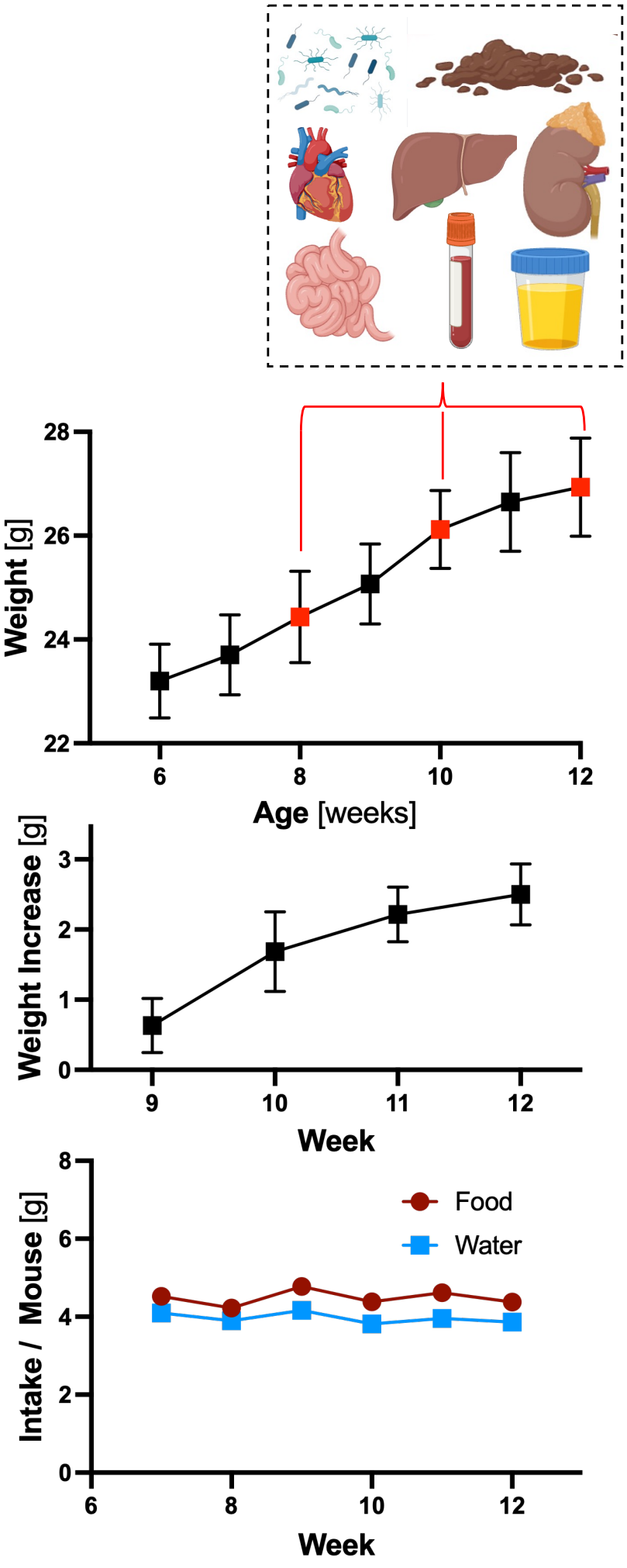

Supplemental Figure 2

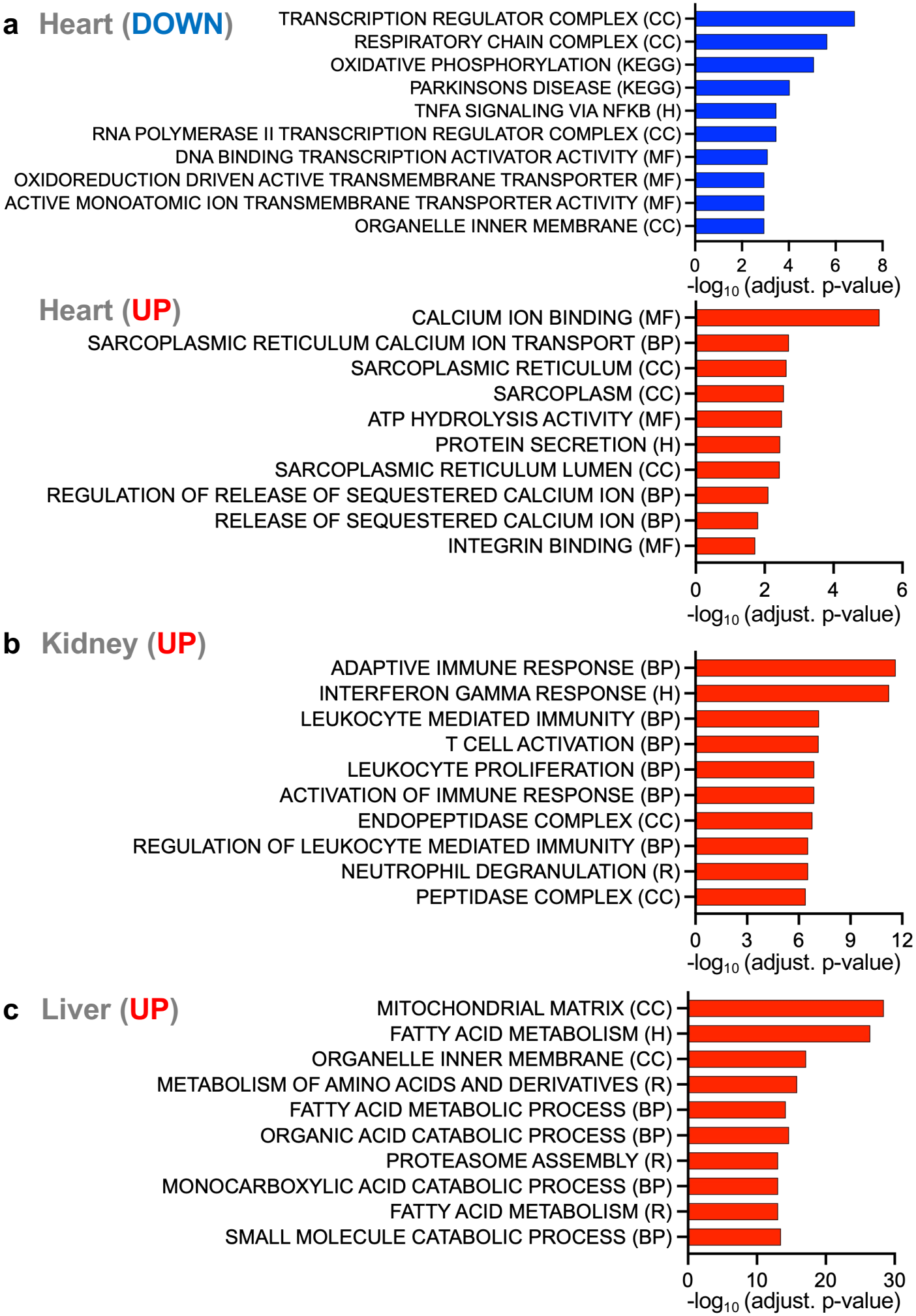

Supplemental Figure 3

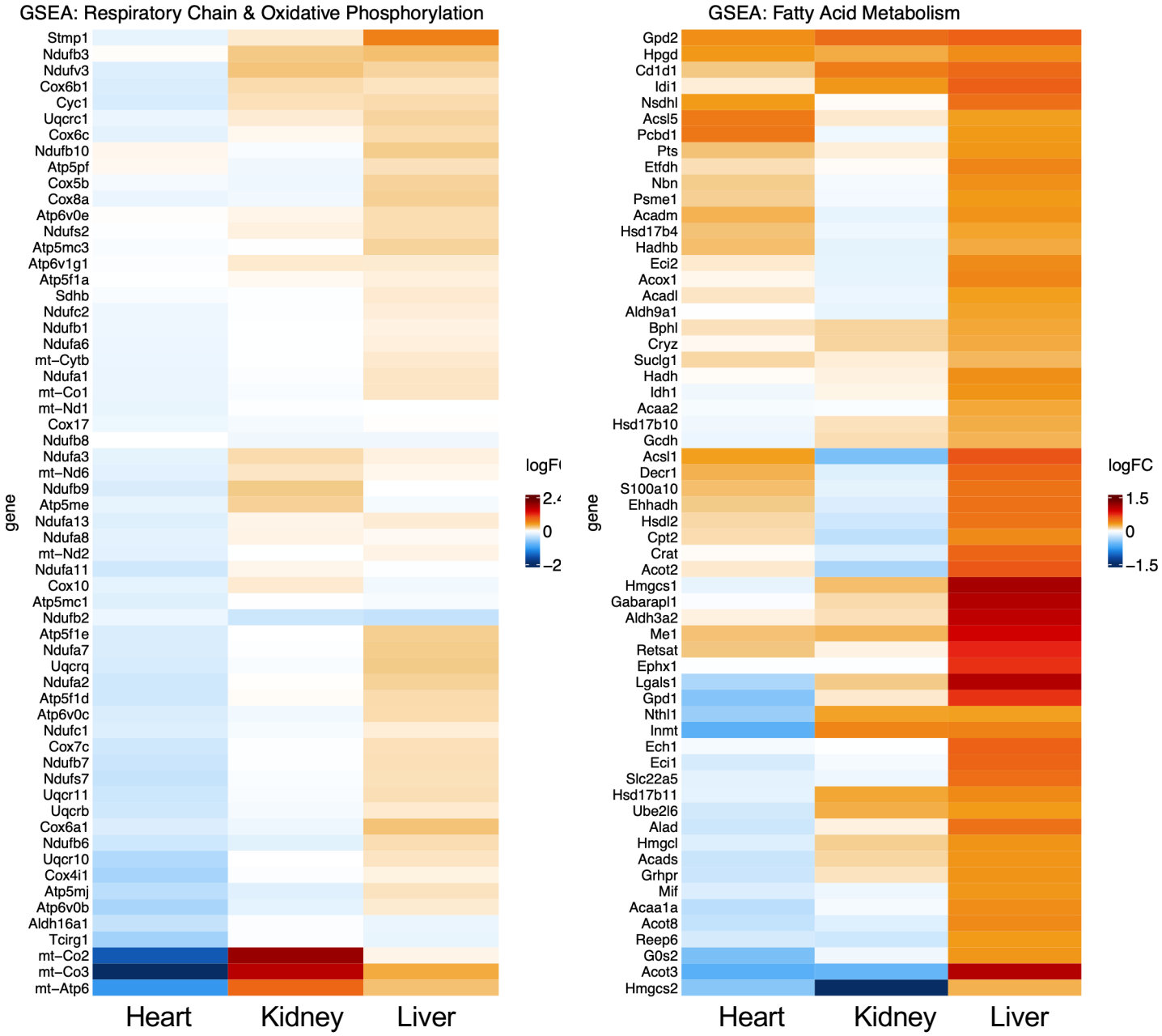

Supplemental Figure 4

a

Intestine | Plasma | Urine

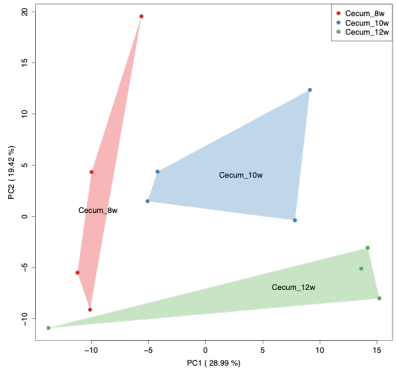

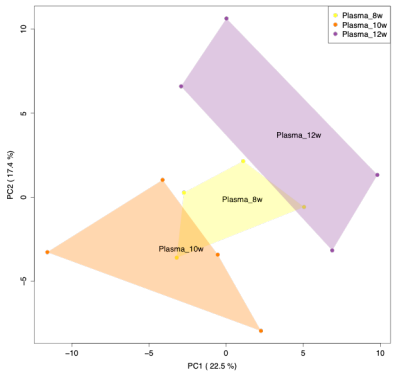

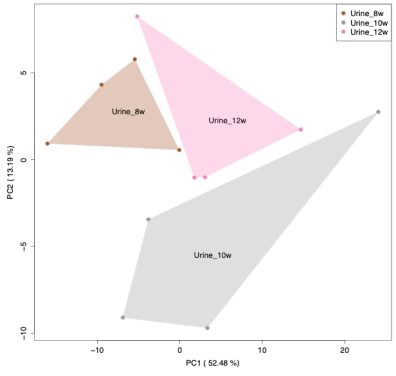

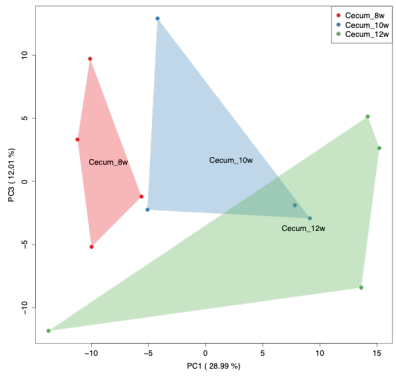

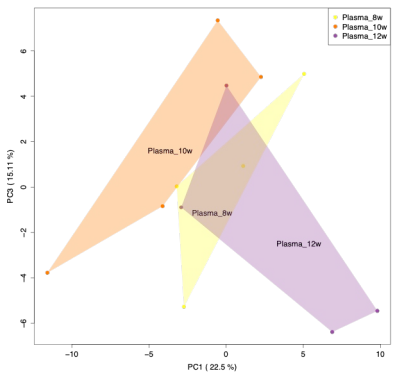

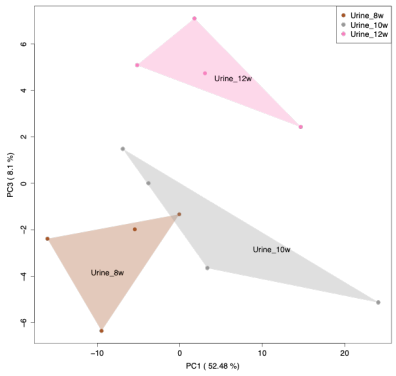

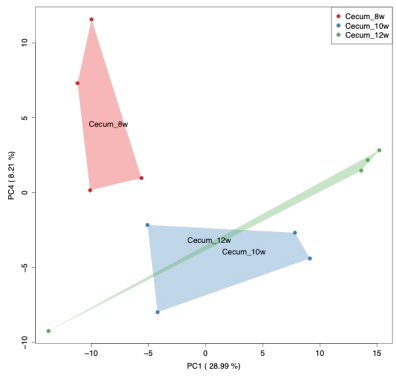

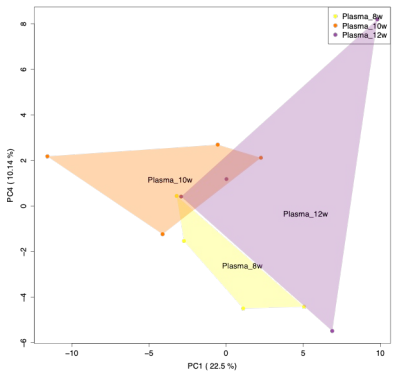

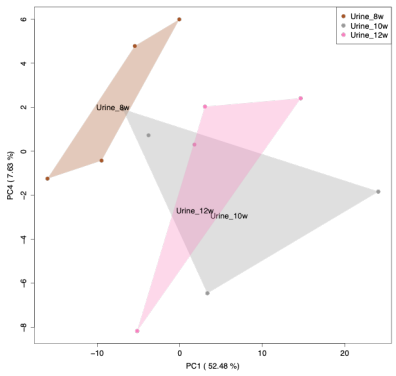

b

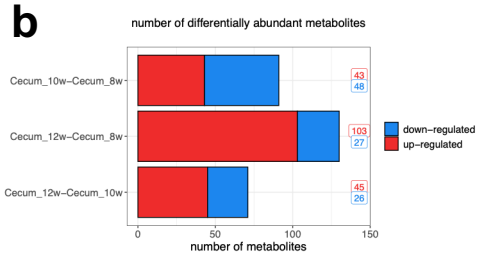

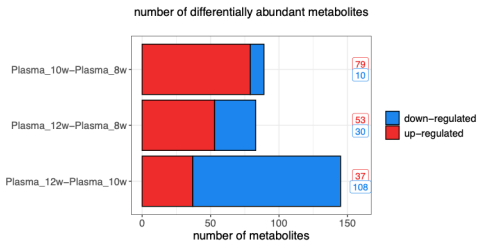

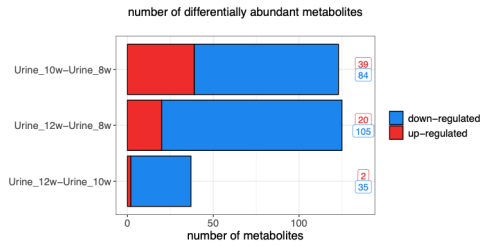

Supplemental Figure 5

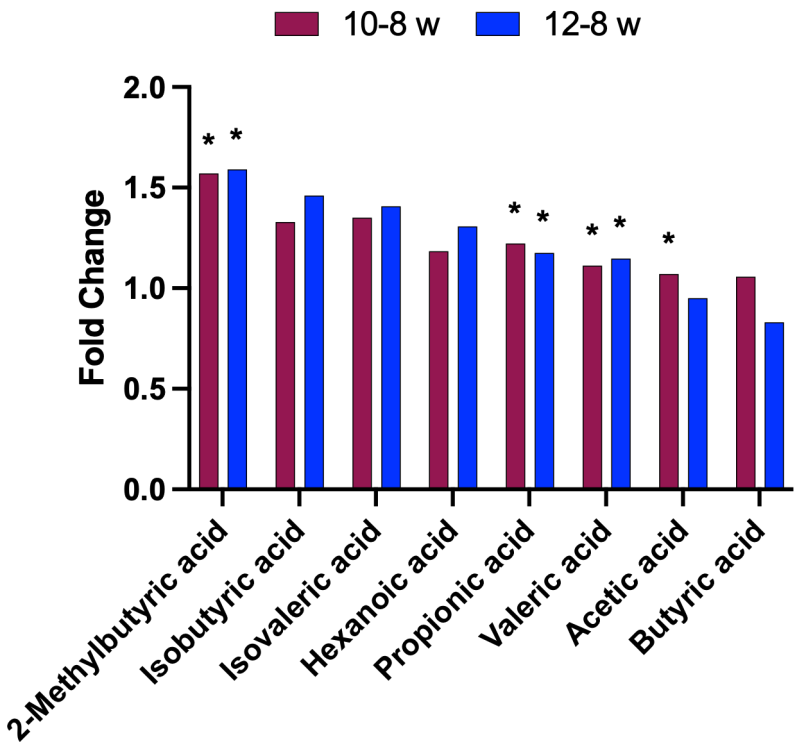

Supplemental Figure 6

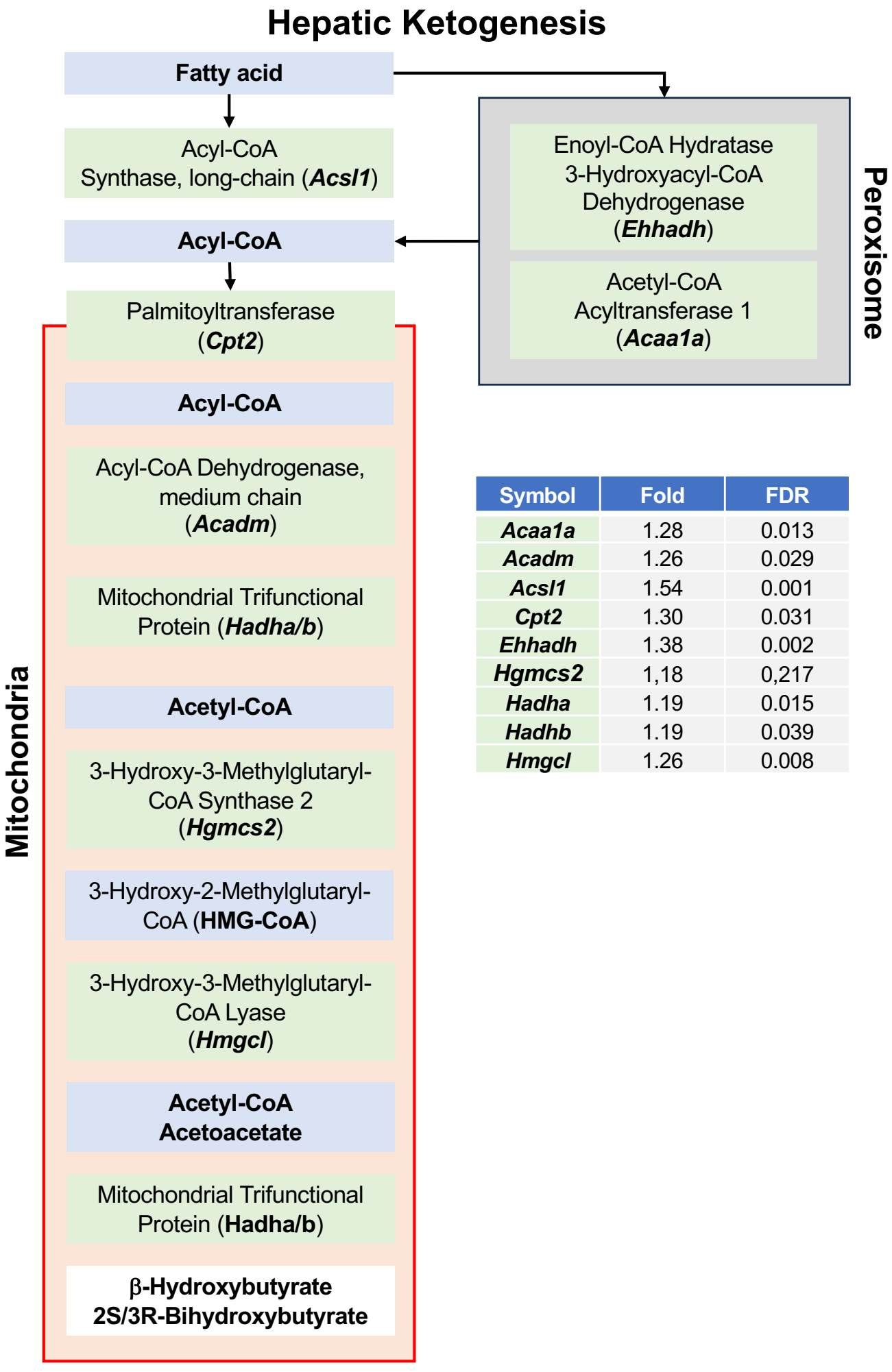

Symbol	Fold	FDR
Acaa1a	1.28	0.013
Acadm	1.26	0.029
Acsl1	1.54	0.001
Cpt2	1.30	0.031
Ehhadh	1.38	0.002
Hgmcs2	1,18	0,217
Hadha	1.19	0.015
Hadhb	1.19	0.039
Hmgcl	1.26	0.008

Supplemental Figure 7

a

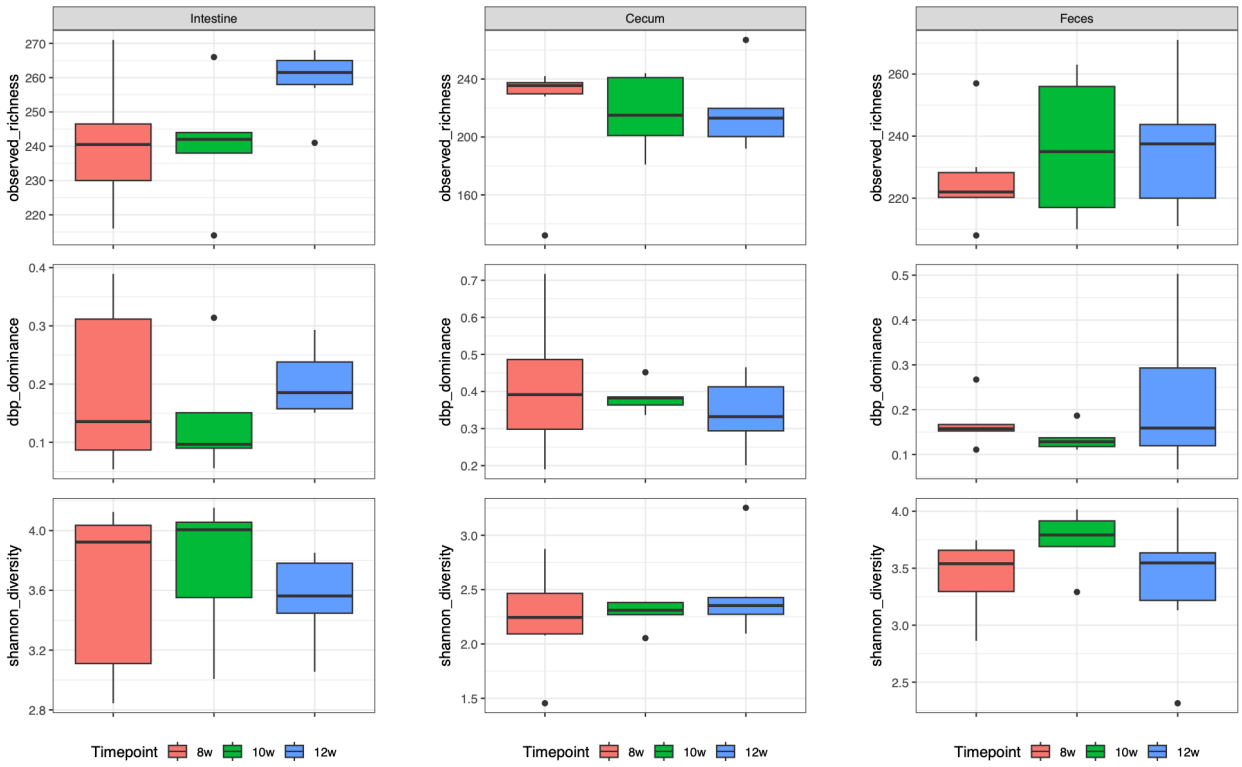

b Small Intestine

Class Order Family Genus *Species*

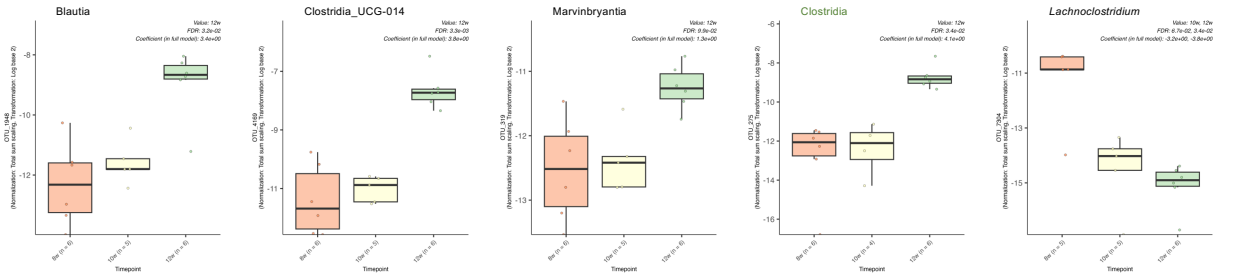

Feces

Class Order Family Genus *Species*